

This discussion paper is/has been under review for the journal Atmospheric Chemistry and Physics (ACP). Please refer to the corresponding final paper in ACP if available.

Stratosphere–troposphere exchange (STE) in the vicinity of North Atlantic cyclones

P. Reutter¹, B. Škerlak², M. Sprenger², and H. Wernli²

¹Institute for Atmospheric Physics, University of Mainz, Mainz, Germany

²Institute for Atmospheric and Climate Science, ETH Zurich, Zürich, Switzerland

Received: 18 December 2014 – Accepted: 12 January 2015 – Published: 27 January 2015

Correspondence to: P. Reutter (preutter@uni-mainz.de)

Published by Copernicus Publications on behalf of the European Geosciences Union.

ACPD

15, 2535–2575, 2015

STE in the vicinity of North Atlantic cyclones

P. Reutter et al.

Title Page	
Abstract	Introduction
Conclusions	References
Tables	Figures
◀	▶
◀	▶
Back	Close
Full Screen / Esc	
Printer-friendly Version	
Interactive Discussion	



Abstract

It is well known that the storm tracks are a preferred region of stratosphere–troposphere exchange (STE), but a systematic and climatological investigation of the connection between cyclones and STE has not yet been performed. We use two established ERA-

- 5 Interim climatologies of STE and cyclones for the years 1979–2011 to quantify the amount of STE that occurs during the life cycle of North Atlantic cyclones. A Lagrangian method serves to identify individual STE events, and a sophisticated cyclone identification tool detects cyclones, their shape and size from the sea-level pressure field. Combining the two data sets reveals that roughly half of the total STE in the North
- 10 Atlantic occurs in the vicinity of cyclones and that both downward and upward fluxes of mass across the tropopause (STT and TST, respectively) are more intense in deeper cyclones (lower minimum pressure) compared to less intense cyclones. In summer, STT and TST in the vicinity of cyclones are almost equal; in the other seasons, STT is larger by 15–45 %. Cross-tropopause mass fluxes are enhanced by a factor of about
- 15 two compared to climatology when a cyclone is present. On average, STE is strongest during the mature phase of cyclones, i.e., in a 24 h time window around the time of maximum intensity. Systematic patterns of exchange locations relative to the cyclone centre are identified via composite analysis and shed light on the different characteristics of STT and TST. During cyclone intensification and in the mature stage, TST is
- 20 mainly confined to the cyclone centre, whereas STT occurs mainly in a region further southwest. During the decay of the cyclones, both STT and TST are most frequent close the cyclone centre, in a region with a fairly low tropopause.

1 Introduction

25 The exchange of air across the extratropical tropopause plays an important role for the chemical composition of the stratosphere and the troposphere. For instance, the injection of stratospheric air into the troposphere can enhance the ozone concentration

ACPD

15, 2535–2575, 2015

STE in the vicinity of North Atlantic cyclones

P. Reutter et al.

Title Page	
Abstract	Introduction
Conclusions	References
Tables	Figures
◀	▶
◀	▶
Back	Close
Full Screen / Esc	
Printer-friendly Version	
Interactive Discussion	



in the troposphere significantly (e.g., Danielsen, 1968; Stevenson et al., 2006), even down to the boundary layer (Johnson and Viezee, 1967; Davies and Schuepbach, 1994; Lefohn et al., 2011; Lin et al., 2012; Škerlak et al., 2014a). On the other side, the amount of water vapour in the extratropical lower stratosphere can strongly increase 5 when tropospheric air is transported across the tropopause (e.g., Stohl et al., 2003; Krebsbach et al., 2006). Even polluted air from the boundary layer can be transported into the extratropical lower stratosphere (e.g., Arnold et al., 1997; Chen et al., 2012). It is therefore relevant to understand and quantify the physical processes leading to 10 and the flow features associated with stratosphere–troposphere exchange (STE) in the extratropics.

In this study, as in many previous studies (e.g., Holton et al., 1995; Stohl et al., 2003), the extratropical tropopause is defined as an isosurface of potential vorticity (PV). Typical values best representing the dynamical transport barrier lie in the range of 1–4 pvu 15 (1 pvu = $10^{-6} \text{ Km}^2 \text{ kg}^{-1} \text{ s}^{-1}$) (see e.g., Kunz et al., 2011) with 2 pvu being a commonly used value (see e.g., Škerlak et al., 2014a). Therefore, as a consequence of the material conservation of PV for adiabatic and frictionless flow (Ertel, 1942; Kleinschmidt, 1950), STE must be associated with processes that lead to a material production or 20 destruction of PV such as cloud microphysical processes (e.g., latent heating due to condensation), radiation, or friction (e.g., associated with turbulence). Furthermore, these physical processes occur preferentially in the vicinity of certain dynamical flow 25 features. This distinction between processes and features is important: processes refer to the physical mechanisms that change PV, whereas features refer to the meteorological flow setting wherein these processes (likely a combination thereof) occur. In the last decades, the processes and flow structures associated with STE have been intensively investigated, as discussed in the review articles by Reiter (1975); Holton et al. (1995); and Stohl et al. (2003). Different studies highlighted the importance of different processes, for instance turbulence by shear instability (Shapiro, 1980; Lamarque and Hess, 1994; Traub and Lelieveld, 2003), the breaking of gravity waves (Whiteway et al., 2003; Wang, 2003; Lane and Sharman, 2006), cloud diabatic processes in stratiform

STE in the vicinity of
North Atlantic
cyclones

P. Reutter et al.

[Title Page](#)[Abstract](#)[Introduction](#)[Conclusions](#)[References](#)[Tables](#)[Figures](#)[◀](#)[▶](#)[◀](#)[▶](#)[Back](#)[Close](#)[Full Screen / Esc](#)[Printer-friendly Version](#)[Interactive Discussion](#)

Title Page	
Abstract	Introduction
Conclusions	References
Tables	Figures
◀	▶
◀	▶
Back	Close
Full Screen / Esc	
Printer-friendly Version	
Interactive Discussion	

and convective clouds (Wirth, 1995; Poulida et al., 1996; Gray, 2003; Bourqui, 2006), and radiative cooling due to strong vertical humidity gradients near the tropopause (Zierl and Wirth, 1997). Regarding flow features, a strong focus has been on STE in tropopause folds that occur near the polar and subtropical jets (Danielsen, 1968; 5 Vaughan et al., 1994; Sprenger et al., 2003; Škerlak et al., 2014b). The first of these studies investigated the exchange processes in a fold in detail, also using airborne radioactivity measurements. Sprenger et al. (2003) compiled a one-year climatology of folds and showed that for STE in the subtropics, folds are highly important (around 60 % of total STE occurs near folds), whereas in the extratropics, where folds are comparatively rare, they only account for about 20 % of total STE. Using a similar approach, 10 Sprenger et al. (2007) quantified the importance of isentropic PV streamers and cut-offs, resulting from Rossby wave breaking, for STE and found that about 70 % of all STE events between 290 and 350 K occur in the vicinity of such a PV feature¹. In the current study, the occurrence of STE in the feature category of extratropical cyclones 15 is quantified.

Several studies in the last decade used global reanalysis data to provide a climatological picture of STE (Seo and Bowman, 2001; Sprenger and Wernli, 2003; James et al., 2003; Berthet et al., 2007; Škerlak et al., 2014a). Most of them are based on Lagrangian methods, which allow diagnosing STE based on PV-changes along kinematic 20 trajectories (Wernli and Davies, 1997; Wirth and Egger, 1999; Wernli and Bourqui, 2002). These climatologies indicate that the distribution of STE in the extratropics has a strong seasonal cycle and pronounced geographic variability. In particular, it was shown that maxima of STE are located over the storm track regions in the North Atlantic and North Pacific during all seasons (except summer) with an averaged mass flux 25 of approximately $500 \text{ kg km}^{-2} \text{ s}^{-1}$ from the stratosphere to the troposphere (STT) and approximately $300 \text{ kg km}^{-2} \text{ s}^{-1}$ in the opposite direction (TST) (Škerlak et al., 2014a).

¹Note that the different features categories are not mutually exclusive; for instance, a tropopause fold can occur as part of a PV cutoff, and therefore the sum of the percentages associated with different features can exceed 100 %.

This indicates qualitatively that STE is likely enhanced in the vicinity of cyclones compared to the climatological average.

Previous studies estimated the amount of STE in the vicinity of individual cyclones by considering idealized baroclinic waves (Bush and Peltier, 1994) or real case studies (e.g. Bourqui, 2006). Some of them then extrapolated their results to the global scale. Due to the considerable variability of cyclone life-cycles and their associated STE processes, this approach is highly uncertain, indicating the need for a systematic climatological investigation. However, these case studies nicely reveal the complex spatio-temporal structures and diverse physical processes associated with STE in cyclones, as briefly summarized here. A first pioneering case study of STE in an extratropical cyclone by Lamarque and Hess (1994) considered a moderately intense winter cyclone over the US and emphasized that the PV perspective is ideal for identifying the physical processes leading to the exchange. For the cyclone considered, they concluded that diabatic processes were much more important than diffusive processes. Intense TST occurred mainly in the western part of the associated upper-level PV structure and STT in the eastern part (i.e., above the cyclone warm sector). A second pioneering case study considered an explosively deepening cyclone (Spaete et al., 1994) and found a similar spatial distribution of STT and TST relative to the cyclone centre. For a North Atlantic winter cyclone, also of moderate intensity, Wernli and Davies (1997) found intense STT during the 24 h of cyclone intensification and much weaker STT during the previous and subsequent days. TST was generally weaker but increased with time and balanced STT on the last day of the cyclone life cycle. TST mainly occurred near the cyclone centre and further north, whereas STT peaked to the rear of the cyclone and along the cold front. Wirth and Egger (1999) used different methods to quantify STE in a decaying Mediterranean cutoff cyclone in summer and showed that convective heating in the centre of the cyclone was mainly responsible for intense STT. Later, Bourqui (2006) considered a similar system in autumn and confirmed the dominance of STT over TST for cyclones associated with an upper-level cutoff. Another study on STE in a cutoff cyclone over Northeast China by Liu et al. (2013) used satellite

STE in the vicinity of North Atlantic cyclones

P. Reutter et al.

[Title Page](#)

[Abstract](#)

[Introduction](#)

[Conclusions](#)

[References](#)

[Tables](#)

[Figures](#)

[◀](#)

[▶](#)

[◀](#)

[▶](#)

[Back](#)

[Close](#)

[Full Screen / Esc](#)

[Printer-friendly Version](#)

[Interactive Discussion](#)



date to quantify the irreversible transport of stratospheric ozone into the troposphere. For a North Atlantic winter cyclone and using a passive tracer in a mesoscale model, Gray (2003) also highlighted the role of deep convection for producing intense STT, however along the long trailing cold front. This is in agreement with the later studies

- 5 by Brioude et al. (2006), who looked at STE in the extratropical transition of tropical storm *Arthur* and pointed to the possible role of deep convection for mixing stratospheric air in folded regions irreversibly into the troposphere, and the investigation of trace gas measurements in several warm season North Atlantic cyclones by Cooper et al. (2002), who emphasized the dry intrusion airstream, which often goes along with 10 a tropopause fold in the rear of an extratropical cyclone, as a preferred region for STT. In contrast, Kowol-Santen et al. (2000) concluded that turbulence in a tropopause fold was more important for STE than cloud diabatic processes. Their study object was 15 a pronounced PV streamer in winter, which broke up into an upper-level cutoff and was associated at its northern end with a surface cyclone over Iceland and further south with a mesocyclone near Portugal. Also using a Lagrangian approach, Sigmund et al. (2000) quantified STE in a stationary North Sea spring cyclone and found STT mainly in a folded upper-level trough and TST in the upper-level ridge. For an intense 20 North American cyclone in early winter, Olsen and Stanford (2001) used trajectories and identified STT due to latent heating in the cyclone centre and due to turbulence further south. This brief summary of case studies of STE in various types of cyclones very clearly highlights the great case-to-case variability of the main processes leading 25 to STE and their preferred location within the cyclonic system. Also the quantitative estimates of STE provided by these case studies are very variable.

To investigate the details of the relationship between STE and North Atlantic cyclones, we combine a climatology of extratropical cyclones based on the identification 25 of closed sea level pressure (SLP) contours (Wernli and Schwierz, 2006) with a recently published climatology of STE (Škerlak et al., 2014a) based on a large set of kinematic trajectories. By combining these climatologies – which are both derived from the ERA-Interim reanalysis data set provided by the European Centre of Medium-

Title Page	
Abstract	Introduction
Conclusions	References
Tables	Figures
◀	▶
◀	▶
Back	Close
Full Screen / Esc	
Printer-friendly Version	
Interactive Discussion	



Range Weather Forecasts (ECMWF) (Dee et al., 2011) – the following questions can be addressed:

- What percentage of the total STT and TST mass flux occurs in the vicinity of extratropical cyclones? What is the regional and seasonal variability of this number?
 - Does STT and TST associated with an individual cyclone depend on its intensity, as expressed by its minimum SLP?
 - Are there, on average, preferred locations for STT and TST within cyclones?
 - What is the timing of STE with respect to the evolution of the cyclone, i.e., is STE more intense during cyclone intensification, in the mature stage, or during decay?
- Answering these questions requires sophisticated methods (e.g., to relate individual STE events to cyclones and to a specific phase of their evolution), which are presented in Sect. 2. Section 3 first shows an illustrative case study of a cyclone and its associated STE, and in Sect. 4 the findings of combining the cyclone and STE climatologies are presented. In Sect. 5 the results are summarized and an outlook is given.

15 2 Data and methods

2.1 ERA-Interim

We use the ERA-Interim reanalysis data set from the European Centre of Medium-Range Weather Forecasts (ECMWF) (Dee et al., 2011). It is based on a 4-D-Var data assimilation technique and is available every 6 h. In this study, we analyse the first 33 yr from 1979 to 2011. The data is available at a T255 spectral grid which corresponds to approximately 80 km. We interpolate all data on a regular grid with 1° resolution in the zonal and meridional directions. The 60 vertical hybrid sigma-pressure model levels reach from the surface up to 0.1 hPa. We compute secondary variables such as potential vorticity (PV) and potential temperature (Θ) directly on the model levels.

[Title Page](#)

[Abstract](#)

[Introduction](#)

[Conclusions](#)

[References](#)

[Tables](#)

[Figures](#)

◀

▶

◀

▶

[Back](#)

[Close](#)

[Full Screen / Esc](#)

[Printer-friendly Version](#)

[Interactive Discussion](#)



2.2 Cyclone identification tool

Extratropical cyclones are identified based on the method described in Wernli and Schwierz (2006). Isobars of sea-level pressure (SLP) are considered at 0.5 hPa intervals between 920 and 1050 hPa and then the regions within closed isobars are accepted as cyclone regions if they additionally fulfill the following criteria: (i) the local minimum of SLP within the enclosing contour is not located over topography exceeding 1500 m height; and (ii) the length of the enclosing contour is smaller than 7500 km, hence excluding unrealistically large features that typically go along with very flat pressure distributions. The first criterion makes sure that spurious SLP minima due to reduction to sea level are excluded from the climatology. The resulting cyclone climatology is a data set of pairs $(C_{\min}, C_{\text{reg}})$ where C_{\min} is defined as the location (longitude and latitude) of the cyclone centre and C_{reg} is a region attributed to this cyclone, defined by the outermost enclosing isobar and represented by a 0/1 label field on the 1° resolution grid.

Use is made of both cyclone features: C_{\min} is needed as input for the cyclone tracking and, e.g., for the composite analysis in Sect. 3.4. The cyclone region C_{reg} is required to attribute every STE event unambiguously to a cyclone, i.e., an STE event “belongs” to a cyclone if it occurs within its associated cyclone region. Note that here we make use of the flow-dependent size attribution of cyclones: our approach can distinguish between smaller and larger cyclones in comparison to a more static approach, which would use, e.g., a constant cyclone radius. However, a complication arises for multi-centre cyclones, where nearby local pressure minima are found within the same enclosing isobar. Since the two minima likely belong to two different cyclone tracks, it is important, in this case, to split the cyclone region between the different centres according to their relative depth.

As mentioned above, cyclone centres at individual times are combined into time-continuous cyclone tracks, as also described in Wernli and Schwierz (2006). Further refinements to the tracking algorithm, as already invoked for the IMILAST cyclone iden-

ACPD

15, 2535–2575, 2015

STE in the vicinity of North Atlantic cyclones

P. Reutter et al.

Title Page	
Abstract	Introduction
Conclusions	References
Tables	Figures
◀	▶
◀	▶
Back	Close
Full Screen / Esc	
Printer-friendly Version	
Interactive Discussion	



STE in the vicinity of North Atlantic cyclones

P. Reutter et al.

[Title Page](#)

[Abstract](#)

[Introduction](#)

[Conclusions](#)

[References](#)

[Tables](#)

[Figures](#)

[◀](#)

[▶](#)

[◀](#)

[▶](#)

[Back](#)

[Close](#)

[Full Screen / Esc](#)

[Printer-friendly Version](#)

[Interactive Discussion](#)



2.4 Combination of cyclone and STE data

To compute the STE mass flux associated with a specific cyclone, we select the STE trajectories that cross the tropopause within the cyclone area defined by the outermost closed SLP contour (see above). Since each trajectory represents a certain mass

5 $\Delta m \approx \frac{1}{g} \Delta x \Delta y \Delta p = 6.52 \times 10^{11}$ kg, this allows us to compute mass fluxes in both directions separately (Δx , Δy and Δp represent the spacing of the trajectory starting points in the horizontal and vertical directions, respectively). Note that this approach is fully dynamic in the sense that for a small cyclone the STE event must occur close to the cyclone centre in order to be associated with the cyclone, whereas for large cyclones an

10 STE event can also be associated with the cyclone if its location is fairly distant from the cyclone centre. In some cases (see below), the adopted definition of the cyclone area might appear a bit too restrictive, i.e., the cyclone area might rather indicate a conservative estimate of the region dynamically influenced by the cyclone evolution. Therefore our estimates of STE attributed to cyclones should also be regarded as a conservative

15 estimate or lower bound. Also, for every STE event classified as associated to a cyclone, the coordinates relative to the cyclone centre are determined, which later allows producing composites of STT and TST relative to the cyclone centre.

3 Introductory case study: cyclone “Xynthia” in February 2010

In this section, we will show a case study to illustrate our methods.

20 3.1 A synoptic scale perspective

We have chosen the winter storm “Xynthia”, which caused severe storm surges and flooding in Western Europe in February 2010 (Liberato et al., 2013). This long-lived cyclone originated in the subtropical North Atlantic near 55°W, intensified explosively and reached the French Atlantic coast with a core pressure of about 970 hPa at 00:00 UTC

[Title Page](#)

[Abstract](#)

[Introduction](#)

[Conclusions](#)

[References](#)

[Tables](#)

[Figures](#)

◀

▶

◀

▶

[Back](#)

[Close](#)

[Full Screen / Esc](#)

[Printer-friendly Version](#)

[Interactive Discussion](#)



STE in the vicinity of North Atlantic cyclones

P. Reutter et al.

[Title Page](#)

[Abstract](#)

[Introduction](#)

[Conclusions](#)

[References](#)

[Tables](#)

[Figures](#)

◀

▶

◀

▶

[Back](#)

[Close](#)

[Full Screen / Esc](#)

[Printer-friendly Version](#)

[Interactive Discussion](#)



28 February (Fig. 1). The cyclone then moved to the Baltic Sea, weakened, became stationary and persisted until 8 March. The situation at 06:00 UTC 26 February 2010 is shown in Fig. 2. A large number of STT events occur right at the cyclone centre (near 30°W/30°N, central pressure 998 hPa). A vertical cross-section along 30°W from 15° to 45°N is shown in Fig. 3. The strong baroclinic zone to the north of the cyclone is not associated with a tropopause fold. A closer analysis (not shown) reveals that most of these STT events can be associated with material PV destruction above a local latent heating maximum due to in-cloud freezing. Note also the STE events associated with the subtropical jet stream over North Africa shown in Fig. 2. At 00:00 UTC 5 27 January 2010, Xynthia has moved north-eastward and significant STT occurs on its north-western side (Fig. 4) in a region with a rather low tropopause (reaching down to 400 hPa). These exchange events, however, are not associated to the cyclone by our method since they occur outside the outermost closed SLP contour (gray area in Fig. 4). This illustrates how our method only takes into account exchange events that 10 occur in the direct vicinity of the cyclone centre. This example shows that we use a conservative estimate of the cyclone area in order to obtain a trustworthy lower bound of STE attributed to cyclones.

3.2 STE integrated along cyclone track

Time series of sea level pressure and exchanged mass for STT and TST events for 20 cyclone “Xynthia” are presented in Fig. 1. This shall illustrate the combination of the cyclone and STE data. The sea level pressure shows the three different phases of the life cycle of a cyclone. During the intensification phase, the sea level pressure is reduced rapidly by over 30 hPa in 72 hours. In the mature phase the minimum pressure of 968.98 hPa is reached, which defines the intensity of “Xynthia”. The minimum pressure is reached 78 h after the first detection of the cyclone by the tracking algorithm. After the mature stage, the sea level pressure rises and the cyclone decays slowly. “Xynthia” is last found by the tracking algorithm after 288 h of overall lifetime, which is an exceptionally long life time for a North Atlantic cyclone. The grey boxes in Fig. 1 25

STE in the vicinity of North Atlantic cyclones

P. Reutter et al.

[Title Page](#)

[Abstract](#)

[Introduction](#)

[Conclusions](#)

[References](#)

[Tables](#)

[Figures](#)

[◀](#)

[▶](#)

[◀](#)

[▶](#)

[Back](#)

[Close](#)

[Full Screen / Esc](#)

[Printer-friendly Version](#)

[Interactive Discussion](#)



indicate the intensification (–36 to –12 hrs prior to the time of minimum pressure) and the decaying phase (12 to 36 hrs after the time of minimum pressure), respectively. Note, to have comparable time windows for all cyclones, regardless of their lifetime, the intensification and decaying phases are limited to 24 h. The mature phase of the cyclone is defined as the time window 12 hrs before and after the time the minimum is reached and is indicated by the yellow box in Fig. 1.

The exchanged masses of STT and TST for each 6 hourly time step are shown as blue and red lines in Fig. 1, respectively. In the beginning of the lifecycle, no STE events are found in the vicinity of “Xynthia”. STT is dominant during the intensification and mature phase of the cyclone, while TST becomes more important in the long decaying phase of “Xynthia”. In the end, the total exchanged mass for STT accounts to 4.25×10^{14} kg and for TST to 7.12×10^{14} kg.

This above mentioned method is now applied to all North Atlantic cyclones from 1979 to 2011 and the results are presented in the following.

15 4 Climatology

4.1 Fraction of STE associated with cyclones

The seasonally averaged mass fluxes of STT and TST in the North Atlantic are shown in Figs. 5 and 6, respectively. The white contours indicate the percentage of the total mass flux that is due to exchange events associated with cyclones. The highest relative fraction (around 70 %) is found for STT south of Greenland in winter (DJF). In spring (MAM) and fall (SON), around 60 % of the total STT flux is associated with cyclones in this region while in summer (JJA), this value drops to 40 %. The values for TST are approximately 10 percentage points lower throughout the year but the patterns are comparable to the ones for STT. Note, that the percentage values are large where the cyclones typically become mature, large and stationary (e.g., between Greenland and Iceland). In the mature stage, cyclones tend to be more barotropic, i.e., the main

upper-level disturbance becomes vertically aligned with the surface low and therefore it makes sense that in this stage a lot of the STE occurs within the cyclone masks. In contrast, in the early phase of the cyclones' life cycles, e.g., in the western North Atlantic, the cyclones typically have a westward tilt with height, i.e., the upper-level intrusions develop upstream of the surface cyclones and as an effect the fraction of STE associated with cyclones is smaller in these regions.

4.2 Influence of cyclone intensity

In this section, we investigate the climatological relationship between STE in the vicinity of North Atlantic cyclones and their intensity. The intensity of a cyclone is defined as the minimum pressure of the cyclone during its lifecycle. All cyclones in the period investigated in this study (1979–2011) are grouped into bins with a width of 5 hPa, ranging from 930 hPa to 1035 hPa. In Fig. 7, the dependency of the exchanged mass per cyclone on the cyclone intensity is shown using box-and-whisker plots for STT and TST in winter (DJF) and summer (JJA). The median of each pressure bin is given by the bold black line, 50% of the data are within the box and the whiskers (dashed lines) denote the 1.5 interquartile range. The statistical outliers are marked as circles.

For winter and summer and for both directions (STT and TST) a clear dependence of the exchanged mass on the minimum pressure of the cyclone can be seen. With decreasing minimum pressure, more mass is exchanged between stratosphere and troposphere along the cyclone track. In winter (DJF) more mass is exchanged for STT than for TST, especially for cyclones with higher intensities, i.e., lower minimum pressure. The STE values integrated along the track of cyclone "Xynthia" (core pressure of 969 hPa), portrayed previously in Fig. 1, are relatively high for STT (0.44×10^{15} kg) compared to the statistical distribution shown in Fig. 7 (top left) and exceptionally high for TST (0.71×10^{15} kg), i.e., in the range of the statistical outliers.

During the summer months (JJA) more mass is exchanged for TST than for STT. Also, the variability of the results is increasing with decreasing minimum pressure, indicated by the larger boxes in each bin, which include 50% of the data. It can also be

[Title Page](#)

[Abstract](#)

[Introduction](#)

[Conclusions](#)

[References](#)

[Tables](#)

[Figures](#)

[◀](#)

[▶](#)

[◀](#)

[▶](#)

[Back](#)

[Close](#)

[Full Screen / Esc](#)

[Printer-friendly Version](#)

[Interactive Discussion](#)



seen that during summer no cyclones with minimum pressure of less than 955 hPa are found.

In Table 1, the total exchanged mass for STT and TST along cyclone tracks and for the complete North Atlantic are listed for all seasons. Spring (MAM, not shown in Fig. 7)

5 shows more exchanged mass for STT, while in fall (SON) both directions of exchange show a more or less equal magnitude.

However, the possibility that the increase of exchanged mass for more intense cyclones is solely due to a longer life time has to be excluded. Therefore, in a next step, the exchanged mass is weighted with the size and the life time of each cyclone to determine the mass flux in the vicinity of a cyclone as a function of its minimum pressure. Figure 8 shows the mass flux per cyclone depending on its minimum pressure. Similar to the total exchanged mass, the mass flux also shows an increase with decreasing minimum pressure of a cyclone. Nevertheless, there are some important differences. The increase of mass flux is not as steep compared to the exchanged mass, because 10 the lifetime and the size of the cyclones are taken into account. Overall, the results show a higher variability which does not strongly depend on the minimum pressure. Note that the variability is clearly higher during winter than during summer. Additionally, the number of outliers (marked by circles) is significantly higher due to very small or 15 very short lived cyclones. During winter, the mass flux is definitely higher for STT than for TST. During summer, however, TST shows a larger mass flux, which is consistent 20 with the results from the total exchanged mass.

Table 2 lists the average mass flux for STT and TST in all seasons. The result show the same characteristics as the exchanged mass (see Table 1) with the highest fluxes in winter for STT. Additionally, winter shows the greatest discrepancy between STT and 25 TST, where the STT flux is 42 % larger than the TST flux. In summer the STT flux is lowest for all seasons, while the TST flux is highest. Overall, the yearly average of the mass flux in the vicinity of a North Atlantic cyclone is $3445 \text{ kg km}^{-2} \text{ s}^{-1}$ for STT and $375 \text{ kg km}^{-2} \text{ s}^{-1}$ for TST, respectively. Comparing these results to the the average mass flux across the tropopause in the entire Northern Hemisphere (approximately $175 \text{ kg km}^{-2} \text{ s}^{-1}$) allows

STE in the vicinity of North Atlantic cyclones

P. Reutter et al.

[Title Page](#)

[Abstract](#)

[Introduction](#)

[Conclusions](#)

[References](#)

[Tables](#)

[Figures](#)

[◀](#)

[▶](#)

[◀](#)

[▶](#)

[Back](#)

[Close](#)

[Full Screen / Esc](#)

[Printer-friendly Version](#)

[Interactive Discussion](#)



to conclude that the mass flux in the vicinity of North Atlantic cyclones is significantly higher compared to cyclone-free regions.

4.3 Position of STE relative to cyclone centre

In addition to a quantitative attribution of STE to cyclones, it is also of interest to study where STE takes place relative to the cyclone centre, i.e. to assess whether there are distinct patterns discernible or if STE is randomly distributed around the centre. To address this question, composites of STE are compiled (Figs. 9 and 10). Our method works as follows: every extra-tropical cyclone is placed in the centre of a rotated longitude/latitude grid and the coordinates of all STE events attributed to this cyclone are then transformed accordingly. Thus, the locations of the STE events are shown relative to the cyclone centre. This is repeated for all cyclones and associated STE events in the climatology, resulting in a STE density around the cyclone centres. Note that the coordinate transformation, placing the cyclone centre at the intersection of the rotated 0° meridian and equator, guarantees that all cyclones and exchange events are treated equivalently. No distortion due to the converging meridians toward the poles occurs and the spacing of 1° in the rotated grid corresponds to ~ 110 km in good approximation. Hence, the domain shown in Figs. 9 and 10 covers an area of approximately 2000 km \times 2000 km around the cyclone centre.

In addition to STE composites relative to the cyclone centre, Figs. 9 and 10 also includes composites of the cyclone mask (see Sect. 2) and of PV at the 315 K isentrope. The former gives a good idea of the horizontal extension of the cyclones included in the composite; the latter shows the upper-level dynamical evolution of the PV field and is hence a proxy of the upper-level forcing of the cyclone. At the same time, by definition, this field also shows the mean position of the dynamical tropopause at this isentropic level. Finally, note that in Figs. 9 and 10, only cyclones in the North Atlantic region which deepen by at least 10 hPa during their lifetime are considered (see Sect. 2). The results are presented for three different stages of the cyclones life cycle; (i) 36 to 12 h before the minimum pressure is reached (intensification phase), (ii) 12 h before and

Title Page	
Abstract	Introduction
Conclusions	References
Tables	Figures
◀	▶
◀	▶
Back	Close
Full Screen / Esc	
Printer-friendly Version	
Interactive Discussion	



12 h after the time of maximum intensity (mature phase), and (iii) 12 to 36 h after the minimum pressure (decaying phase). Additionally, for each phase of the life cycle the mass flux for STT and TST is shown.

- With respect to STT (Fig. 9, second row) several distinct features are discernible:
- 5 (i) During the intensification phase (left), most STT takes place in a sector south-west of the cyclone centre. The maximum is found well within the mean cyclone mask and resembles a rectangle of nearly $400\text{ km} \times 300\text{ km}$ width. In this intensification phase, the PV contours also indicate a clear structure, where the highest PV values are reminiscent of a stratospheric PV trough to the north-west of the cyclone centre. (ii) During
 - 10 the mature phase (Fig. 9, middle column), the pattern changes: the STT maximum is shifted further to the south and significant STT can now also be found to the south-east of the cyclone centre. The shift in the STT pattern goes along with a clear evolution of PV at 315K. In fact, the PV signal is indicative for cyclonic rolling-up of the upper-level PV trough. (iii) This evolution becomes most pronounced in the decaying phase (right column). Here, the averaged upper-level PV has formed a distinct, nearly axisymmetric PV cutoff situated exactly over the cyclone centre. The distribution of STT becomes much more symmetric, and is also located near the cyclone centre. Furthermore, the horizontal extent of regions with substantial STT is strikingly reduced compared to the previous two time periods considered.

- 20 The magnitude of the exchanged STT mass (Fig. 9, first row) is also changing with time. The dependence of the mass on the minimum pressure (based on the complete life cycle) is visible for all life cycle stages. However, the lowest exchanged mass can be found during the intensification phase. The exchanged STT mass is highest when the cyclones reach their minimum pressure. This is the time when the geographical distribution of the STT events shows the largest asymmetry. Here, most of the STT mass exchange occurs south of the cyclone centre, where the highest wind speeds of Northern Hemisphere extratropical cyclones are expected. In the decaying phase the exchanged mass is reduced, but slightly higher compared to the intensification phase.

Title Page	
Abstract	Introduction
Conclusions	References
Tables	Figures
◀	▶
◀	▶
Back	Close
Full Screen / Esc	
Printer-friendly Version	
Interactive Discussion	



A similar analysis can be repeated with respect to TST (Fig. 10, second row). Again the same time windows of the cyclones' lifetimes are considered (from left to right) and the same cyclones are included in the composites. Compared to the STT pattern, the TST pattern is much more spatially confined and axisymmetrically distributed around the cyclone centre. Especially in the intensification and mature phase, the TST decays rapidly for distances larger than ≈ 250 km away from the centre. There is a slight indication of a small geographical shift toward the south-east from the intensification to the mature phase, most likely associated with the corresponding evolution of the upper-level PV signal. Indeed, in the intensification phase the highest number of TST events are found in a narrow region on the downstream side of the PV trough; at minimum pressure, however, the peak TST is found right below the rolling-up PV trough. During the decaying phase (right) the horizontal extension of the TST widens and is slightly shifted to the south-west of the cyclone centre, nearly perfectly aligned with the upper-level PV signal.

The exchanged TST mass is shown in Fig. 10 (first row). The evolution of the exchanged mass between the different time windows is clearly not varying as much as for the STT mass. In all life stages an increase of exchanged TST mass with decreasing minimum pressure is visible. However, the overall exchanged mass for each individual pressure class is only slightly increased during the period of minimum pressure, which is in contrast to the STT mass at this time. It is noticeable that the increased exchanged STT mass coincides with the asymmetry of the geographical distribution of the exchange events. In contrast, the geographical pattern of the TST exchange events is more or less symmetric through all life stages.

5 Conclusions, discussion and outlook

In this study we investigated stratosphere–troposphere exchange in the vicinity of extratropical cyclones over the North Atlantic. A chain of sophisticated tools and methods based on ERA-Interim data enabled us to obtain a detailed attribution of individual

ACPD

15, 2535–2575, 2015

STE in the vicinity of North Atlantic cyclones

P. Reutter et al.

Title Page	
Abstract	Introduction
Conclusions	References
Tables	Figures
◀	▶
◀	▶
Back	Close
Full Screen / Esc	
Printer-friendly Version	
Interactive Discussion	



STE events to a particular cyclone track in the extratropical North Atlantic from 1979 to 2011. A case study of a winter cyclone was presented to illustrate the methods and conceptual approach. The results of the climatological investigations are summarized and discussed in the following.

5 5.1 Main results

5.1.1 Fraction of STE associated with cyclones

As indicated by earlier case studies summarized in the introduction, STE is typically enhanced in the vicinity of extratropical cyclones. STE in cyclones therefore contributes significantly to total STE and this has been quantified for the first time in this study for 10 the North Atlantic storm track. The highest fraction of STE associated with cyclones compared to all STE events over the North Atlantic can be found during winter, when up to 70 % of the STT mass flux occurs near cyclones. In spring and fall, this value drops to around 60 %. The lowest fraction can be found during summer, when less than 50 % of the STT mass flux can be attributed to cyclones. The values for the TST 15 mass flux are similarly distributed but approximately 10 percentage points lower than the values of STT throughout the year.

5.1.2 Influence of cyclone intensity on STE

The exchanged mass across the tropopause in the vicinity of a cyclone is strongly dependent on the cyclone intensity, expressed as the minimum SLP during its lifecycle. 20 With increasing cyclone intensity (i.e., lower minimum SLP), the spatially and temporally integrated STT and TST mass fluxes along the cyclone tracks are enhanced. In winter, the dependency is stronger for STT than for TST. During summer, both directions of exchange have a comparable dependency on the intensity.

When considering the averaged mass flux along a cyclone track, i.e., dividing the 25 integrated exchange values by the size and lifetime of the cyclone, the results show

ACPD

15, 2535–2575, 2015

STE in the vicinity of North Atlantic cyclones

P. Reutter et al.

[Title Page](#)

[Abstract](#)

[Introduction](#)

[Conclusions](#)

[References](#)

[Tables](#)

[Figures](#)

[◀](#)

[▶](#)

[◀](#)

[▶](#)

[Back](#)

[Close](#)

[Full Screen / Esc](#)

[Printer-friendly Version](#)

[Interactive Discussion](#)



the same overall behaviour. However, the variability of the data within the intensity classes is increasing due to the variability of size and lifetime of North Atlantic cyclones. On average, the STT mass flux for a cyclone with a minimum SLP of 1000 hPa in winter (summer) is approximately $240 \text{ kg km}^{-2} \text{ s}^{-1}$ ($160 \text{ kg km}^{-2} \text{ s}^{-1}$), and for a cyclone with a minimum SLP of 960 hPa the corresponding average flux amounts to $400 \text{ kg km}^{-2} \text{ s}^{-1}$ ($350 \text{ kg km}^{-2} \text{ s}^{-1}$). The TST mass flux for a winter (summer) cyclone with a minimum core pressure of 1000 hPa is about $175 \text{ kg km}^{-2} \text{ s}^{-1}$ ($250 \text{ kg km}^{-2} \text{ s}^{-1}$), and for a cyclone with a minimum core pressure of 960 hPa about $350 \text{ kg km}^{-2} \text{ s}^{-1}$ ($375 \text{ kg km}^{-2} \text{ s}^{-1}$). Note that the dependency of the averaged mass flux on the cyclone intensity is weaker compared to the integrated exchanged mass. The reason for the dependency of the exchanged mass (or mass flux) on the intensity of cyclones is difficult to unravel from a climatological study alone. A very strong hypothesis is that the increase in exchanged mass with increasing cyclone intensity is associated with enhanced diabatic processes, in particular latent heat release in clouds, and potentially also the infrared cooling at cloud top level. Climatological studies on cyclone intensification (e.g., Čampa and Wernli, 2012) clearly showed that latent heating is enhanced in strongly intensifying cyclones. This is corroborated by climatological studies of rainfall in extratropical cyclones, which show an increase of surface precipitation for more intense cyclones (Field and Wood, 2007). Since process studies (e.g., Lamarque and Hess, 1994, and others discussed in the introduction) highlighted the importance of the diabatic PV modification for STE, it is very likely that the same diabatic processes leading to cyclone intensification also increase the cross-tropopause mass exchange. In addition, the tropopause near intense cyclones is typically very low (Čampa and Wernli, 2012) and often forms filaments reaching deep into the troposphere. It is conceivable that the strong vertical wind shear in these regions results in more turbulence and hence more exchange.

STE in the vicinity of
North Atlantic
cyclones

P. Reutter et al.

[Title Page](#)[Abstract](#)[Introduction](#)[Conclusions](#)[References](#)[Tables](#)[Figures](#)[◀](#)[▶](#)[◀](#)[▶](#)[Back](#)[Close](#)[Full Screen / Esc](#)[Printer-friendly Version](#)[Interactive Discussion](#)

5.1.3 Position of STE relative to cyclone centre

Composites of STE exchange locations relative to the cyclone centre were obtained to assess differences in the spatial distribution of STT and TST events. In the intensification phase most STT occurs south-west of the cyclone centre. This pattern moves to the south of the cyclone centre when the cyclone reaches its maximum intensity (minimum pressure). In the decaying phase the STT pattern becomes much more axisymmetric and is located right above the cyclone centre. It is notable that the pattern of STT goes along with the PV anomaly at 315 K indicating a cyclonic roll-up of the upper-level PV trough. In contrast, the TST pattern is much more spatially confined and axisymmetric. In the intensification phase the TST pattern is centred slightly downstream of the upper-level trough. However, during the mature phase of the cyclone the maximum of the TST pattern is aligned below the rolling-up PV trough. In the decaying phase the pattern of TST widens and is located south-west of the cyclone centre.

5.1.4 STE with respect to the evolution of a cyclone

The timing of STE with respect to the cyclone lifecycle shows some differences for STT and TST. Both show the highest amount of exchanged mass during the time of the cyclones maximum intensity. However, the median mass flux for STT at that time is clearly higher and the variability is significantly increased. The higher variability of the STT is also present in the intensification and decaying phases of the cyclone. Additionally, the median of the STT is slightly higher in the decaying phase compared to the intensification phase. The exchanged TST mass in the intensification and decaying phases are equally strong, but overall weaker than the exchanged STT mass. As mentioned above, it is remarkable that the variability of the TST mass is always significantly lower compared to the STT mass. This leads to the assumption that the intensity of a cyclone is a more robust measure for TST than for STT. The results for STT suggest that other parameters of the cyclone play also an important role in governing the mass flux from the stratosphere to the troposphere.

STE in the vicinity of North Atlantic cyclones

P. Reutter et al.

[Title Page](#)

[Abstract](#)

[Introduction](#)

[Conclusions](#)

[References](#)

[Tables](#)

[Figures](#)

[◀](#)

[▶](#)

[◀](#)

[▶](#)

[Back](#)

[Close](#)

[Full Screen / Esc](#)

[Printer-friendly Version](#)

[Interactive Discussion](#)



5.2 Caveats

Several caveats concerning the data set and the methods are discussed in the following.

5.2.1 STE in ERA-Interim data set

- 5 The calculation of STE due to sub-grid-scale convective processes, which could be of importance in the vicinity of cyclones, is not possible using kinematic trajectories based on resolved wind fields in ERA-Interim reanalysis data. Therefore, the mass flux across the tropopause is probably underestimated. However, a quantification of this underestimation cannot be given using the presented method. For further information
10 see also Škerlak et al. (2014a) and references therein.

5.2.2 Size of cyclones

The size of the cyclone determines how many STE events are associated with it. Therefore, different definitions of the size will lead to different quantifications of the cross-tropopause transport assigned to a cyclone. As it was shown in the case study in

- 15 Sect. 3, situations can occur where a large number of STE events are not attributed to a cyclone, because they are not within the outermost closed contour of SLP, although the distance of the exchange to the cyclone centre is small. This could be avoided by using a fixed radius around the cyclone centre. However, this method then would ignore the individual characteristics of a cyclone.

20 5.2.3 Cyclone track

While the definition of a cyclone affects its size, the identification of the cyclone track affects the lifetime and adds an uncertainty into the quantitative results of the exchanged mass (mass flux) per cyclone. An intercomparison of 15 different detection and tracking tools for extratropical cyclones (Neu et al., 2013) revealed that uncertainties are most

ACPD

15, 2535–2575, 2015

STE in the vicinity of North Atlantic cyclones

P. Reutter et al.

[Title Page](#)

[Abstract](#)

[Introduction](#)

[Conclusions](#)

[References](#)

[Tables](#)

[Figures](#)

◀

▶

◀

▶

[Back](#)

[Close](#)

[Full Screen / Esc](#)

[Printer-friendly Version](#)

[Interactive Discussion](#)



notable for weak cyclones. However, the methods agreed well for cyclones in oceanic regions and also reproduced similar geographical patterns of cyclone frequency. Using a different method might therefore change the quantitative results of the investigation, but not the overall conclusion that there is a strong dependency of the STE flux on cyclone intensity.

5

5.3 STE in future climate

This investigation showed that cyclones play a very important role for extratropical STE. It was found that the exchanged mass (and mass flux) strongly depend on the intensity of a cyclone. It was also found that the preferred locations for STT and TST relative to the cyclone centre as well as their intensity vary between different stages of the cyclone's life cycle.

10

To make a statement on STE in the vicinity of cyclones for a future climate, projections of storm track activity under global warming can be used. Chang et al. (2012) examined storm track changes in the future climate using multi-model ensembles from the Coupled Model Intercomparison Project (CMIP5, Taylor et al., 2012) and found no systematic shift of Northern Hemisphere (NH) storm tracks during the NH winter and only a slight poleward shift during NH summer. Additionally, they found that the cyclone frequency is projected to be smaller over Europe and North America. Also, they noticed that the intensity of the cyclones is slightly decreased. This would lead to an overall decrease in exchanged mass across the tropopause in the vicinity of cyclones, when our results are taken into account. However, it has to be noted that Chang et al. (2012) found that the models generally simulate storm tracks that are too weak. Our results imply that a small deviation in the intensity of a cyclone can lead to a significant under- or overestimation of the STE mass flux. Hence, this implies that models have to be very accurate in their description of the processes governing the life cycle of cyclones in order to project STE in the vicinity of cyclones, and therefore STE in general, properly.

15

20

25

[Title Page](#)

[Abstract](#)

[Introduction](#)

[Conclusions](#)

[References](#)

[Tables](#)

[Figures](#)

[◀](#)

[▶](#)

[◀](#)

[▶](#)

[Back](#)

[Close](#)

[Full Screen / Esc](#)

[Printer-friendly Version](#)

[Interactive Discussion](#)



5.4 Outlook

One way for future studies to gain more insight into the dependency of STE on cyclone intensity is a systematic and detailed climatological evaluation of the processes involved in STE near cyclones with different intensities to test the above-mentioned 5 hypothesis concerning the importance of diabatic processes. One approach could be to retrieve physical tendencies along trajectories within cyclones in order to investigate the influence of diabatic processes depending on cyclone intensity, which could be done from a climatological point of view. Another possibility is to conduct case studies of cyclones with various intensities in order to trace the PV rates of different diabatic 10 processes within the cyclones. Additionally, it would also be worth looking into cases, where cyclones with very different intensities are associated with a similar mass flux (amount of exchanged mass) or, vice versa, cases, where cyclones with similar intensity end up in very different mass fluxes (amount of exchanged mass).

Acknowledgements. We thank MeteoSwiss and the ECMWF for granting access to the ERA-15 Interim data set. P. Reutter thanks P. Spichtinger for helpful discussions.

References

- Arnold, F., Schneider, J., Gollinger, K., Schlager, H., Schulte, P., Hagen, D. E., Whitefield, P. D., and van Velthoven, P.: Observation of upper tropospheric sulfur dioxide- and acetone-pollution: potential implications for hydroxyl radical aerosol formation, *Geophys. Res. Lett.*, 24, 57–60, 1997. 2537
- Berthet, G., Esler, J. G., and Haynes, P. H.: A Lagrangian perspective of the tropopause and the ventilation of the lowermost stratosphere, *J. Geophys. Res.*, 112, D18102, doi:10.1029/2006JD008295, 2007. 2538
- Bourqui, M. S.: Stratosphere–troposphere exchange from the Lagrangian perspective: a case 25 study and method sensitivities, *Atmos. Chem. Phys.*, 6, 2651–2670, doi:10.5194/acp-6-2651-2006, 2006. 2538, 2539

[Title Page](#)[Abstract](#)[Introduction](#)[Conclusions](#)[References](#)[Tables](#)[Figures](#)[◀](#)[▶](#)[◀](#)[▶](#)[Back](#)[Close](#)[Full Screen / Esc](#)[Printer-friendly Version](#)[Interactive Discussion](#)

Brioude, J., Cammas, J.-P., and Cooper, O. R.: Stratosphere–troposphere exchange in a summertime extratropical low: analysis, *Atmos. Chem. Phys.*, 6, 2337–2353, doi:10.5194/acp-6-2337-2006, 2006. 2540

5 Bush, A. B. G. and Peltier, W. R.: Tropopause folds and synoptic-scale baroclinic wave life cycles, *J. Atmos. Sci.*, 51, 1581–1604, doi:10.1175/1520-0469(1994)051<1581:TFASSB>2.0.CO;2, 1994. 2539

Čampa, J. and Wernli, H.: A PV perspective on the vertical structure of mature midlatitude cyclones in the Northern Hemisphere., *J. Atmos. Sci.*, 69, 725–740, 2012. 2553

10 Chang, E. K. M., Guo, Y., and Xia, X.: CMIP5 multimodel ensemble projection of storm track change under global warming, *J. Geophys. Res.*, 117, D23, doi:10.1029/2012JD018578, 2012. 2556

Chen, B., Xu, X. D., Yang, S., and Zhao, T. L.: Climatological perspectives of air transport from atmospheric boundary layer to tropopause layer over Asian monsoon regions during boreal summer inferred from Lagrangian approach, *Atmos. Chem. Phys.*, 12, 5827–5839, doi:10.5194/acp-12-5827-2012, 2012. 2537

15 Cooper, O. R., Moody, J. L., and Parrish, D. D.: Trace gas composition of midlatitude cyclones over the western North Atlantic Ocean: a seasonal comparison of O₃ and CO, *J. Geophys. Res.*, 107, D7, doi:10.1029/2001JD000902, 2002. 2540

20 Danielsen, E. F.: Stratospheric-tropospheric exchange based on radioactivity, ozone and potential vorticity, *J. Atmos. Sci.*, 25, 502–518, doi:10.1175/1520-0469(1968)025<0502:STEBOR>2.0.CO;2, 1968. 2537, 2538

Davies, T. D. and Schuepbach, E.: Episodes of high ozone concentrations at the earth's surface resulting from transport down from the upper troposphere/lower stratosphere: a review and case studies, *Atmos. Environ.*, 28, 53–68, doi:10.1016/1352-2310(94)90022-1, 1994. 2537

25 Dee, D. P., Uppala, S. M., Simmons, A. J., Berrisford, P., Poli, P., Kobayashi, S., Andrae, U., Balmaseda, M. A., Balsamo, G., Bauer, P., Bechtold, P., Beljaars, A. C. M., van de Berg, L., Bidlot, J., Bormann, N., Delsol, C., Dragani, R., Fuentes, M., Geer, A. J., Haimberger, L., Healy, S. B., Hersbach, H., Holm, E. V., Isaksen, L., Kallberg, P., Köhler, M., Matricardi, M., McNally, A. P., Monge-Sanz, B. M., Morcette, J.-J., Park, B.-K., Peubey, C., de Rosnay, P., Tavolato, C., Thepaut, J.-N., and Vitart, F.: The ERA-Interim reanalysis: configuration and performance of the data assimilation system, *Q. J. Roy. Meteor. Soc.*, 137, 553–597, doi:10.1002/qj.828, 2011. 2541

30 Ertel, H.: Ein neuer hydrodynamischer Wirbelsatz, *Meteorol. Z.*, 59, 271–281, 1942. 2537

[Title Page](#)

[Abstract](#)

[Introduction](#)

[Conclusions](#)

[References](#)

[Tables](#)

[Figures](#)

◀

▶

◀

▶

[Back](#)

[Close](#)

[Full Screen / Esc](#)

[Printer-friendly Version](#)

[Interactive Discussion](#)



- Field, P. R. and Wood, R.: Precipitation and cloud structure in midlatitude cyclones, *J. Climate*, 20, 233–254, 2007. 2553
- Gray, S. L.: A case study of stratosphere to troposphere transport: the role of convective transport and the sensitivity to model resolution, *J. Geophys. Res.*, 108, 4590, doi:10.1029/2002JD003317, 2003. 2538, 2540
- Holton, J. R., Haynes, P. H., McIntyre, M. E., Douglass, A. R., Rood, R. B., and Pfister, L.: Stratosphere–troposphere exchange, *Rev. Geophys.*, 33, 403–440, doi:10.1029/95RG02097, 1995. 2537, 2543
- Hoskins, B. J., McIntyre, M. E., and Robertson, A. W.: On the use and significance of isentropic potential vorticity maps, *Q. J. Roy. Meteor. Soc.*, 111, 877–946, doi:10.1002/qj.49711147002, 1985. 2543
- James, P., Stohl, A., Forster, C., Eckhardt, S., Seibert, P., and Frank, A.: A 15-year climatology of stratosphere–troposphere exchange with a Lagrangian particle dispersion model: 1. Methodology and validation, *J. Geophys. Res.*, 108, 8519, doi:10.1029/2002JD002637, 2003. 2538
- Johnson, W. B. and Viegze, W.: Stratospheric ozone in the lower troposphere – I. Presentation and interpretation of aircraft measurements, *Atmos. Environ.*, 15, 1309–1323, doi:10.1016/0004-6981(81)90325-5, 1981. 2537
- Kleinschmidt, E.: Über Aufbau und Entstehung von Zyklonen, Teil 1, *Meteorol. Rundsch.*, 3, 1–6, 1950. 2537
- Kowol-Santen, J., Elbern, H., and Ebel, A.: Estimation of cross-tropopause airmass fluxes at midlatitudes: comparison of different numerical methods and meteorological situations, *Mon. Weather Rev.*, 128, 4045–4057, 2000. 2540
- Krebsbach, M., Schiller, C., Brunner, D., Günther, G., Hegglin, M. I., Mottaghay, D., Riese, M., Spelten, N., and Wernli, H.: Seasonal cycles and variability of O_3 and H_2O in the UT/LMS during SPURT, *Atmos. Chem. Phys.*, 6, 109–125, doi:10.5194/acp-6-109-2006, 2006. 2537
- Kunz, A., Konopka, P., Müller, R., and Pan, L. L.: Dynamical tropopause based on isentropic potential vorticity gradients, *J. Geophys. Res.*, 116, 2156–2202, doi:10.1029/2010JD014343, 2011. 2537
- Lamarque, J.-F., and Hess, P. G.: Cross-tropopause mass exchange and potential vorticity budget in a simulated tropopause folding, *J. Atmos. Sci.*, 51, 2246–2246, doi:10.1175/1520-0469(1994)051<2246:CTMEAP>2.0.CO;2, 1994. 2537, 2539, 2553

STE in the vicinity of North Atlantic cyclones

P. Reutter et al.

[Title Page](#)[Abstract](#)[Introduction](#)[Conclusions](#)[References](#)[Tables](#)[Figures](#)[◀](#)[▶](#)[◀](#)[▶](#)[Back](#)[Close](#)[Full Screen / Esc](#)[Printer-friendly Version](#)[Interactive Discussion](#)

Title Page	
Abstract	Introduction
Conclusions	References
Tables	Figures
◀	▶
◀	▶
Back	Close
Full Screen / Esc	
Printer-friendly Version	
Interactive Discussion	



Lane, T. and Sharman, R.: Gravity wave breaking, secondary wave generation, and mixing above deep convection in a three-dimensional cloud model, *Geophys. Res. Lett.*, 33, L23813, doi:10.1029/2006GL027988, 2006. 2537

Lefohn, A. S., Wernli, H., Shadwick, D., Limbach, S., Oltmans, S. J., and Shapiro, M.: The importance of stratospheric-tropospheric transport in affecting surface ozone concentrations in the western and northern tier of the United States, *Atmos. Environ.*, 45, 4845–4857, doi:10.1016/j.atmosenv.2011.06.014, 2011. 2537

Liberato, M. L. R., Pinto, J. G., Trigo, R. M., Ludwig, P., Ordóñez, P., Yuen, D., and Trigo, I. F.: Explosive development of winter storm Xynthia over the subtropical North Atlantic Ocean, *Nat. Hazards Earth Syst. Sci.*, 13, 2239–2251, doi:10.5194/nhess-13-2239-2013, 2013. 2544

Lin, M., Fiore, A. M., Cooper, O. R., Horowitz, L. W., Langford, A. O., Levy, H., Johnson, B. J., Naik, V., Oltmans, S. J., and Senff, C. J.: Springtime high surface ozone events over the western United States: quantifying the role of stratospheric intrusions, *J. Geophys. Res.*, 117, D00V22, doi:10.1029/2012JD018151, 2012. 2537

Liu, C., Liu, Y., Liu, X., and Chance, K.: Dynamical and chemical features of a cutoff low over northeast China in July 2007: results from satellite measurements and reanalysis, *Adv. Atmos. Sci.*, 30, 525–540, 2013. 2539

Neu, U., Akperov, M. G., Bellenbaum, N., Benestad, R., Blender, R., Caballero, R., Co-cozza, A., Dacre, H. F., Feng, Y., Fraedrich, K., Grieger, J., Gulev, S., Hanley, J., Hewson, T., Inatsu, M., Keay, K., Kew, S. F., Kindem, I., Leckebusch, G. C., Liberato, M. L. R., Lionello, P., Mokhov, I. I., Pinto, J. G., Raible, C. C., Reale, M., Rudeva, I., Schuster, M., Simmonds, I., Sinclair, M., Sprenger, M., Tilinina, N. D., Trigo, I. F., Ulbrich, S., Ulbrich, U., Wang, X. L., and Wernli, H.: IMILAST: a community effort to intercompare extratropical cyclone detection and tracking algorithms, *Bull. Amer. Meteor. Soc.*, 94, 529–547, doi:10.1175/BAMS-D-11-00154.1, 2013. 2543, 2555

Olsen, M. and Stanford, J.: Evidence of stratosphere-to-troposphere transport within a mesoscale model and Total Ozone Mapping Spectrometer total ozone, *J. Geophys. Res.*, 106, 27323–27334, 2001. 2540

Poulida, O., Dickerson, R., and Heymsfield, A.: Stratosphere–troposphere exchange in a mid-latitude mesoscale convective complex 1. Observations, *J. Geophys. Res.*, 101, 6823–6836, doi:10.1029/95JD03523, 1996. 2538

Reiter, E. R.: Stratospheric-tropospheric exchange processes, *Rev. Geophys.*, 13, 459–474, doi:10.1029/RG013i004p00459, 1975. 2537

- Seo, K.-H. and Bowman, K. P.: A climatology of isentropic cross-tropopause exchange, *J. Geophys. Res.*, 106, 28159–28172, 2001. 2538
- Shapiro, M. A.: Turbulent mixing within tropopause folds as a mechanism for the exchange of chemical constituents between the stratosphere and troposphere, *J. Atmos. Sci.*, 37, 994–1004, doi:10.1175/1520-0469(1980)037<0994:TMWTFA>2.0.CO;2, 1980. 2537
- 5 Sigmond, M., Meloen, J., and Siegmund, P. C.: Stratosphere–troposphere exchange in an extratropical cyclone, calculated with a Lagrangian method, *Ann. Geophys.*, 18, 573–582, doi:10.1007/s00585-000-0573-1, 2000. 2540
- 10 Škerlak, B., Sprenger, M., and Wernli, H.: A global climatology of stratosphere–troposphere exchange using the ERA-Interim data set from 1979 to 2011, *Atmos. Chem. Phys.*, 14, 913–937, doi:10.5194/acp-14-913-2014, 2014a. 2537, 2538, 2540, 2543, 2555
- Škerlak, B., Sprenger, M., Pfahl, S., Tyrlis, E., and Wernli, H.: Tropopause folds in ERA-Interim: 15 Global climatology and relation to extreme weather events, *J. Geophys. Res. Atmos.*, in review, 2014b. 2538, 2543
- Spaete, P., Johnson, D. R., and Schaack, T. K.: Stratospheric-tropospheric mass exchange during the Presidents' Day Storm., *Mon. Weather Rev.*, 122, 424–439, 1994. 2539
- 20 Sprenger, M. and Wernli, H.: A northern hemispheric climatology of cross-tropopause exchange for the ERA15 time period (1979–1993), *J. Geophys. Res.*, 108, 8521, doi:10.1029/2002JD002636, 2003. 2538
- Sprenger, M., Croci Maspali, M., and Wernli, H.: Tropopause folds and cross-tropopause exchange: a global investigation based upon ECMWF analyses for the time period March 2000 to February 2001, *J. Geophys. Res.*, 108, 8518, doi:10.1029/2002JD002587, 2003. 2538
- 25 Sprenger, M., Wernli, H., and Bourqui, M.: Stratosphere–troposphere exchange and its relation to potential vorticity streamers and cutoffs near the extratropical tropopause, *J. Atmos. Sci.*, 64, 1587–1602, doi:10.1175/JAS3911.1, 2007. 2538
- Stevenson, D. S., Dentener, F. J., Schultz, M. G., Ellingsen, K., van Noije, T. P. C., Wild, O., Zeng, G., Amann, M., Atherton, C. S., Bell, N., Bergmann, D. J., Bey, I., Butler, T., Coafala, J., Collins, W. J., Derwent, R. G., Doherty, R. M., Drevet, J., Eskes, H. J., Fiore, A. M., Gauss, M., Hauglustaine, D. A., Horowitz, L. W., Isaksen, I. S. A., Krol, M. C., Lamarque, J.-F., Lawrence, M. G., Montanaro, V., Müller, J.-F., Pitari, G., Prather, M. J., Pyle, J. A., Rast, S., Rodriguez, J. M., Sanderson, M. G., Savage, N. H., Shindell, D. T., Strahan, S. E., Sudo, K., and Szopa, S.: Multimodel ensemble simulations of present-day and near-future tropospheric ozone, *J. Geophys. Res.*, 111, D08301, doi:10.1029/2005JD006338, 2006. 2537

STE in the vicinity of North Atlantic cyclones

P. Reutter et al.

[Title Page](#)[Abstract](#)[Introduction](#)[Conclusions](#)[References](#)[Tables](#)[Figures](#)[◀](#)[▶](#)[◀](#)[▶](#)[Back](#)[Close](#)[Full Screen / Esc](#)[Printer-friendly Version](#)[Interactive Discussion](#)

Stohl, A., Bonasoni, P., Cristofanelli, P., Collins, W., Feichter, J., Frank, A., Forster, C., Gerassopoulos, E., Gäggeler, H., James, P., Kentarchos, A. S., Kromp-Kolb, H., Krüger, B., Land, C., Meloen, J., Papayannis, A., Priller, A., Seibert, P., Sprenger, M., Roelofs, G. J., Scheel, H. E., Schnabel, C., Siegmund, P., Tobler, L., Trickl, T., Wernli, H., Wirth, V., Zanis, P., and Zerefos, C.: Stratosphere–troposphere exchange: a review, and what we have learned from STACCATO, *J. Geophys. Res.*, 108, 8516, doi:10.1029/2002JD002490, 2003. 2537

Taylor, K. E., Stouffer, R. J., and Meehl, G. A.: An overview of CMIP5 and the experiment design, *B. Am. Meteorol. Soc.*, 93, 485–498, doi:10.1175/BAMS-D-11-00094.1, 2012. 2556

Traub, M. and Lelieveld, J.: Cross-tropopause transport over the eastern Mediterranean, *J. Geophys. Res.*, 108, 4712, doi:10.1029/2003JD003754, 2003. 2537

Vaughan, G., Price, J. D., and Howells, A.: Transport into the troposphere in a tropopause fold, *Q. J. Roy. Meteor. Soc.*, 120, 1085–1103, 1994. 2538

Wang, P.: Moisture plumes above thunderstorm anvils and their contributions to cross-tropopause transport of water vapor in midlatitudes, *J. Geophys. Res.*, 108, D6, doi:10.1029/2002JD002581, 2003. 2537

Wernli, H. and Bourqui, M.: A Lagrangian “1-year climatology” of (deep) cross-tropopause exchange in the extratropical Northern Hemisphere, *J. Geophys. Res.*, 107, 4021, doi:10.1029/2001JD000812, 2002. 2538, 2543

Wernli, H. and Davies, H.: A Lagrangian-based analysis of extratropical cyclones. 1: The method and some applications, *Q. J. Roy. Meteor. Soc.*, 123, 467–489, 1997. 2538, 2539

Wernli, H. and Schwierz, C.: Surface cyclones in the ERA-40 dataset (1958–2001). Part I: Novel identification method and global climatology, *J. Atmos. Sci.*, 63, 2486–2507, doi:10.1175/JAS3766.1, 2006. 2540, 2542

Whiteway, J., Pavelin, E., Busen, R., Hacker, J., and Vosper, S.: Airborne measurements of gravity wave breaking at the tropopause, *Geophys. Res. Lett.*, 30, 2070, doi:10.1029/2003GL018207, 2003. 2537

Wirth, V.: Diabatic heating in an axisymmetric cut-off cyclone and related stratosphere–troposphere exchange, *Q. J. Roy. Meteor. Soc.*, 121, 127–147, doi:10.1002/qj.49712152107, 1995. 2538

Wirth, V. and Egger, J.: Diagnosing extratropical synoptic-scale stratosphere–troposphere exchange: a case study, *Q. J. Roy. Meteor. Soc.*, 125, 635–655, doi:10.1002/qj.49712555413, 1999. 2538, 2539

[Title Page](#)

[Abstract](#)

[Introduction](#)

[Conclusions](#)

[References](#)

[Tables](#)

[Figures](#)

◀

▶

◀

▶

[Back](#)

[Close](#)

[Full Screen / Esc](#)

[Printer-friendly Version](#)

[Interactive Discussion](#)



**STE in the vicinity of
North Atlantic
cyclones**

P. Reutter et al.

Title Page	
Abstract	Introduction
Conclusions	References
Tables	Figures
◀	▶
◀	▶
Back	Close
Full Screen / Esc	
Printer-friendly Version	
Interactive Discussion	

STE in the vicinity of
North Atlantic
cyclones

P. Reutter et al.

Table 1. Total mass [10^{17} kg] per season from 1979 to 2011 for STT and TST in the vicinity of cyclones over the North Atlantic and the total mass over the entire North Atlantic as well as the ratio between STT and TST. The minimum lifetime of a cyclone is one day.

Seasons	near cyclones			North Atlantic		
	STT	TST	STT/TST	STT	TST	STT/TST
DJF	9.1	6.9	1.31	22.0	17.8	1.24
MAM	9.0	7.9	1.14	18.5	16.2	1.14
JJA	7.9	9.0	0.88	15.0	16.4	0.91
SON	9.7	9.2	1.05	19.1	17.6	1.09
TOTAL	35.7	33.0	1.08	74.6	68.0	1.10

STE in the vicinity of
North Atlantic
cyclones

P. Reutter et al.

Table 2. Average mass flux [$\text{kg km}^{-2} \text{ s}^{-1}$] per season from 1979 to 2011 for STT and TST in the vicinity of cyclones over the North Atlantic and the average over the entire North Atlantic as well as the ratio between STT and TST. The minimum lifetime of a cyclone is one day.

Seasons	near cyclones			North Atlantic		
	STT	TST	STT/TST	STT	TST	STT/TST
DJF	583.2	409.9	1.42	311.0	252.0	1.23
MAM	462.4	389.1	1.19	262.1	229.0	1.14
JJA	398.0	420.7	0.95	212.8	231.9	0.92
SON	480.4	420.8	1.14	271.0	248.8	1.09
MEAN	481.0	410.1	1.17	264.2	240.4	1.10

Title Page

Abstract

Introduction

Conclusions

References

Tables

Figures

◀

▶

◀

▶

Back

Close

Full Screen / Esc

Printer-friendly Version

Interactive Discussion



STE in the vicinity of
North Atlantic
cyclones

P. Reutter et al.

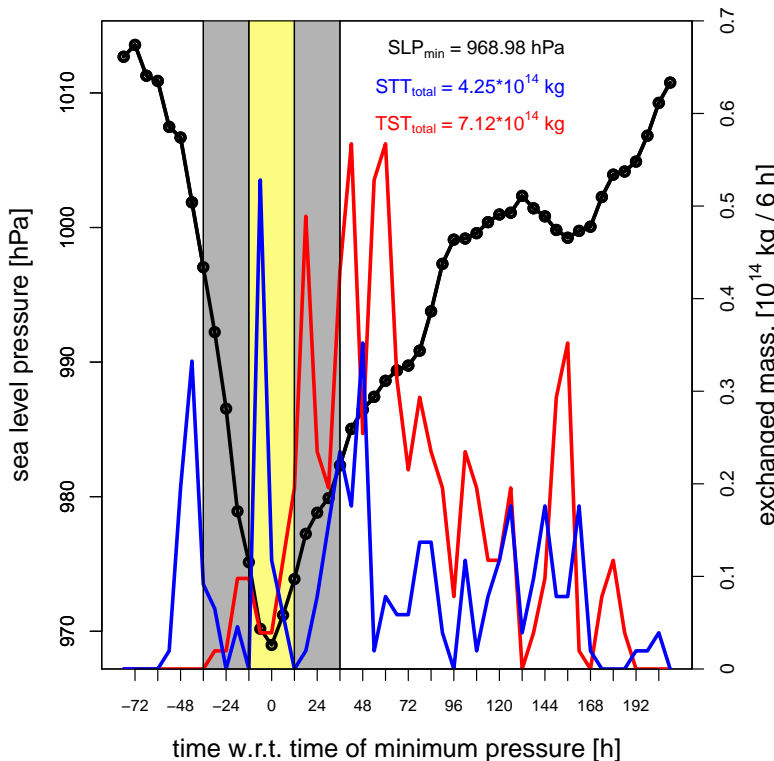


Figure 1. Time series of the sea level pressure (hPa) in black and the exchanged mass (10^{14} kg) of STT (blue) and TST (red) as a function of time (h) with respect to the time of minimum pressure of cyclone "Xynthia". 0h corresponds with 00:00 UTC of 28 February 2010. The grey boxes correspond to the deepening and decaying phase of the cyclone, respectively, and the yellow box indicates the mature phase. The separation into phases is later used for the analysis in Sect. 4.3 (see also Figs. 9 and 10).

STE in the vicinity of
North Atlantic
cyclones

P. Reutter et al.

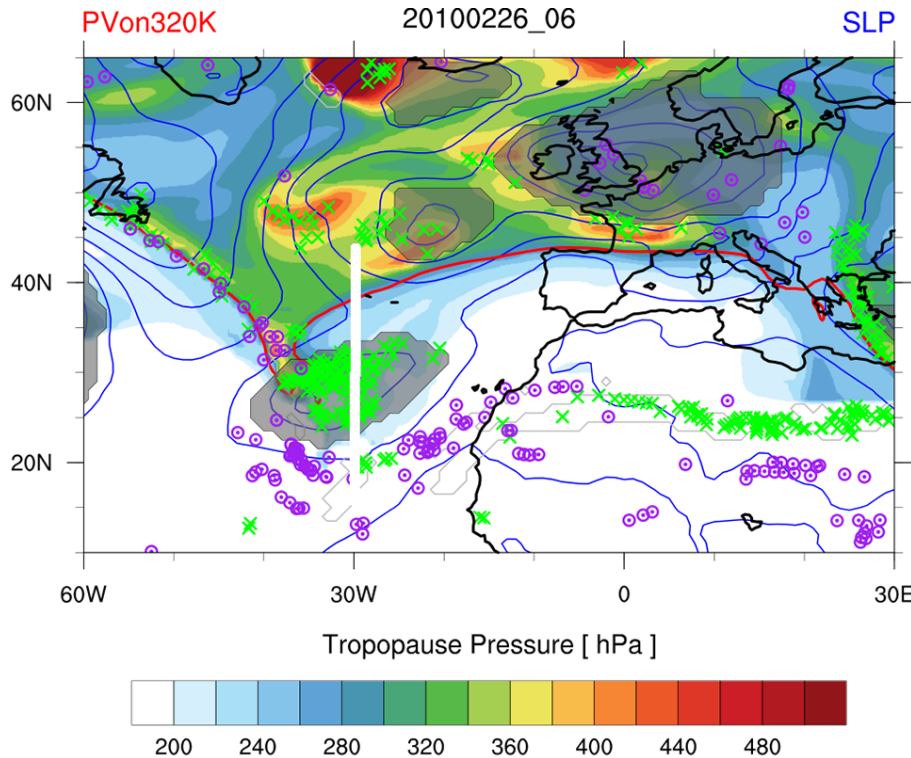


Figure 2. Pressure at the dynamical tropopause (in hPa, coloured), PV at 320 K (red line), and contours of sea-level pressure (blue, contour interval 5 hPa) at 06:00 UTC 26 February 2010. Cyclones, as identified by our method, are shaded gray. STT and TST events occurring within a 6-h symmetric time window are depicted by green crosses and purple dotted circles, respectively. Gray contours indicate a folded tropopause (i.e., multiple vertical crossings).

Figure 3. Vertical cross-section along 30° W from 15 to 45° N (white line in Fig. 2) at 06:00 UTC 26 February 2010. The Brunt–Väisälä frequency N^2 is shown with coloured contours (in 10^{-4} s^{-2}), the thin black lines show isentropes (in K) and the thick contours are isosurfaces of PV (1–4 pvu, 2 pvu red, rest black). STT and TST events occurring in a symmetric 6 h time window and within $\pm 5^\circ$ longitude are shown with green crosses and purple dotted circles, respectively.

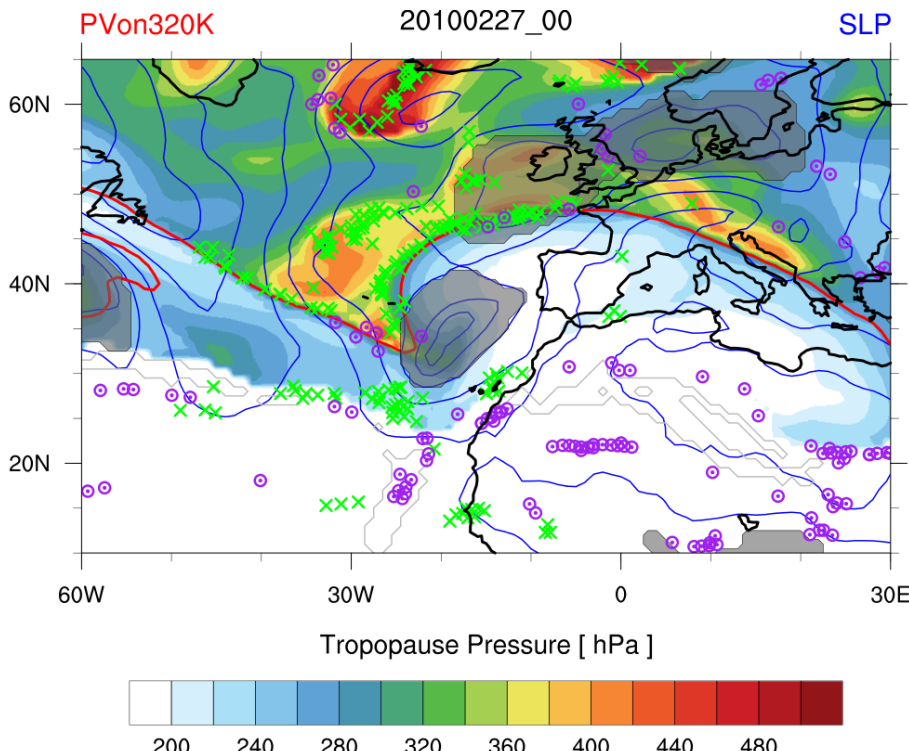


Figure 4. As Fig. 2 but at 00:00 UTC 27 February 2010.

[Printer-friendly Version](#)

Interactive Discussion



STE in the vicinity of
North Atlantic
cyclones

P. Reutter et al.

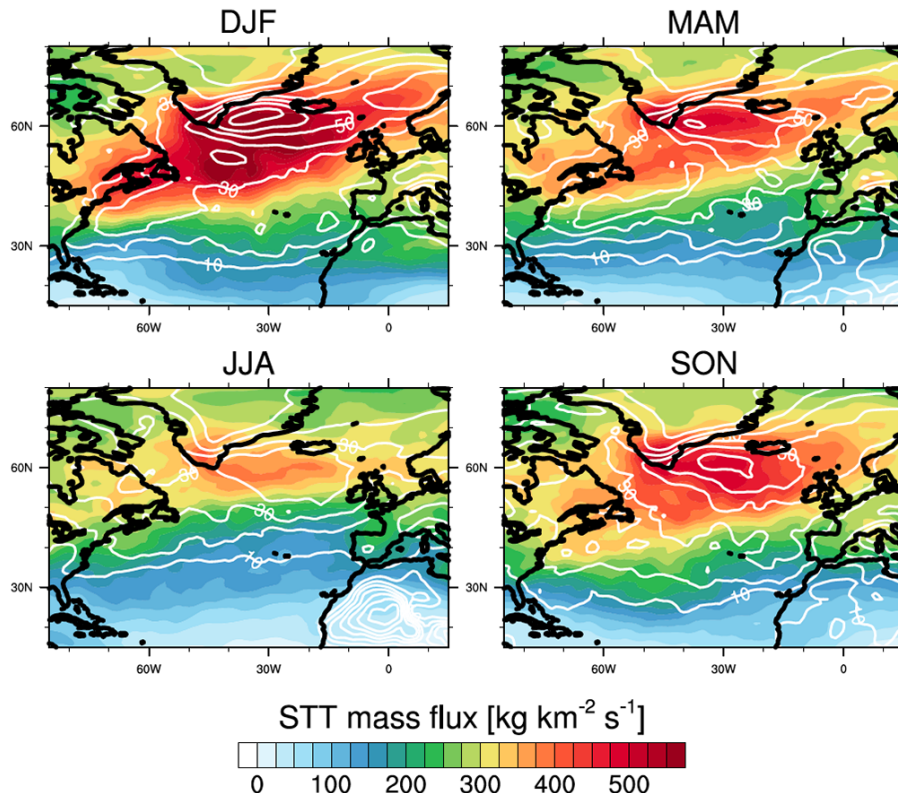


Figure 5. Seasonally averaged STT mass flux for 1979–2011. The white contours indicate the fraction of the mass flux that is associated with cyclones (in %, contour interval 10 %).

**STE in the vicinity of
North Atlantic
cyclones**

P. Reutter et al.

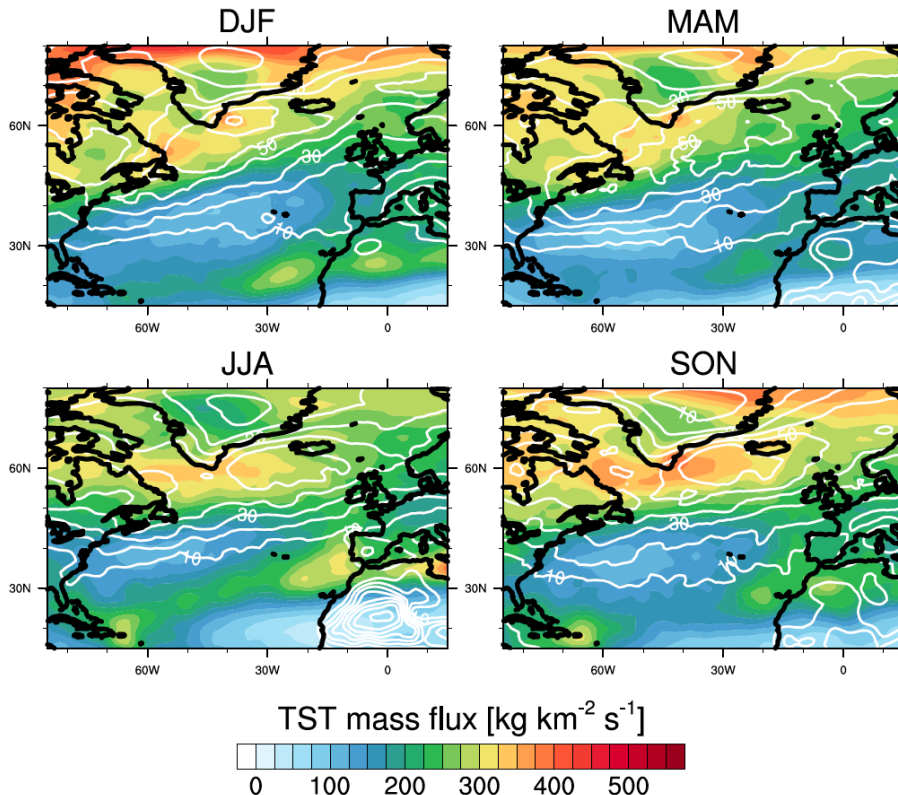


Figure 6. As Fig. 5 but for TST instead of STT.

STE in the vicinity of
North Atlantic
cyclones

P. Reutter et al.

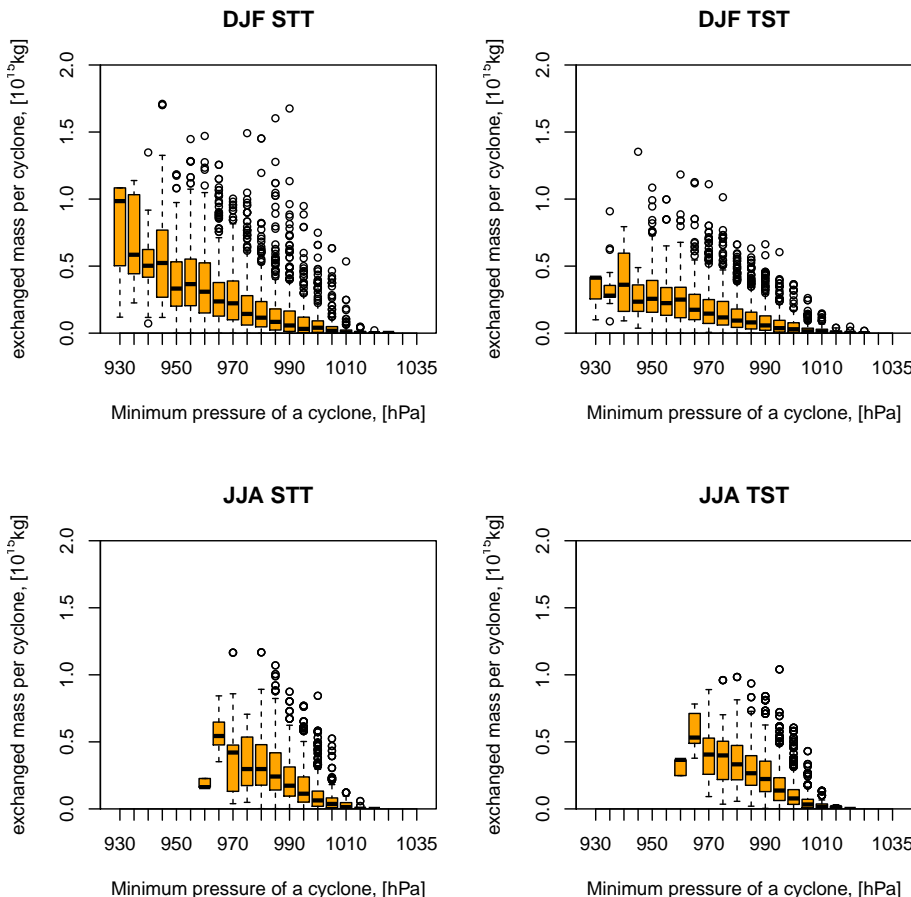


Figure 7. Box-and-Whisker plot showing the dependency of the total exchanged mass per cyclone (10^{15} kg) for STT (left column) and TST (right column) on the minimum pressure of a cyclone (hPa) over the North Atlantic during DJF (upper row) and JJA (lower row).

STE in the vicinity of
North Atlantic
cyclones

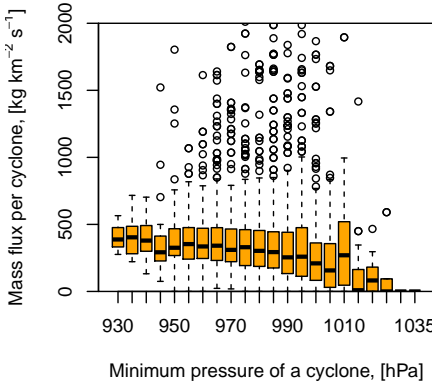
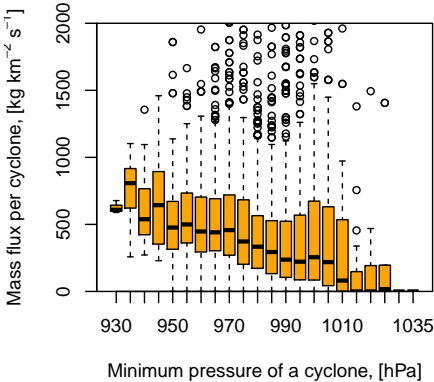
P. Reutter et al.

[Title Page](#)[Abstract](#)[Introduction](#)[Conclusions](#)[References](#)[Tables](#)[Figures](#)[◀](#)[▶](#)[◀](#)[▶](#)[Back](#)[Close](#)[Full Screen / Esc](#)[Printer-friendly Version](#)[Interactive Discussion](#)

Northern Atlantic

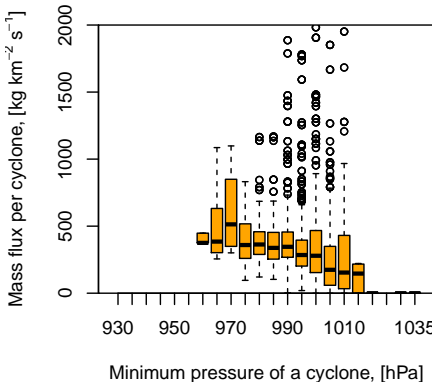
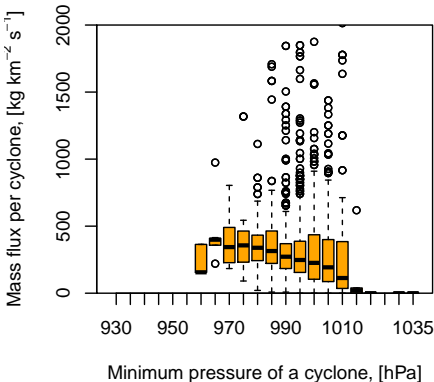
DJF STT

DJF TST



JJA STT

JJA TST

**Figure 8.** As Fig. 7 but for mass flux ($\text{kg km}^{-2} \text{s}^{-1}$)

STE in the vicinity of
North Atlantic
cyclones

P. Reutter et al.

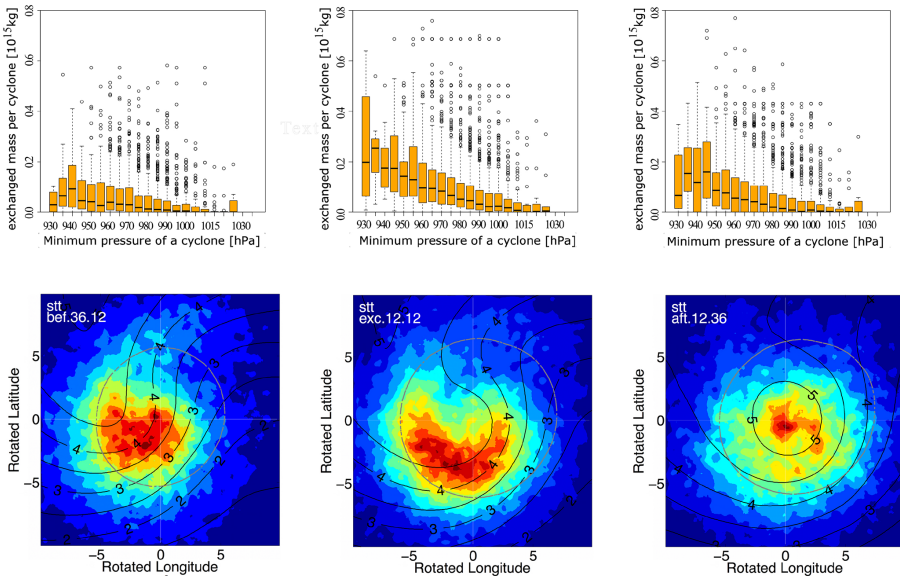


Figure 9. Box and Whisker plots for exchanged mass of STT (first row) and PV- and exchange composites relative to cyclone centre for STT (second row) for the winter months (DJF). Black lines denote PV at 315 K, colouring shows the density of exchange events, the grey line shows the mean extension of a cyclone. The left column shows the result for the intensification phase, the middle column for the mature phase and the right column for the decaying phase.

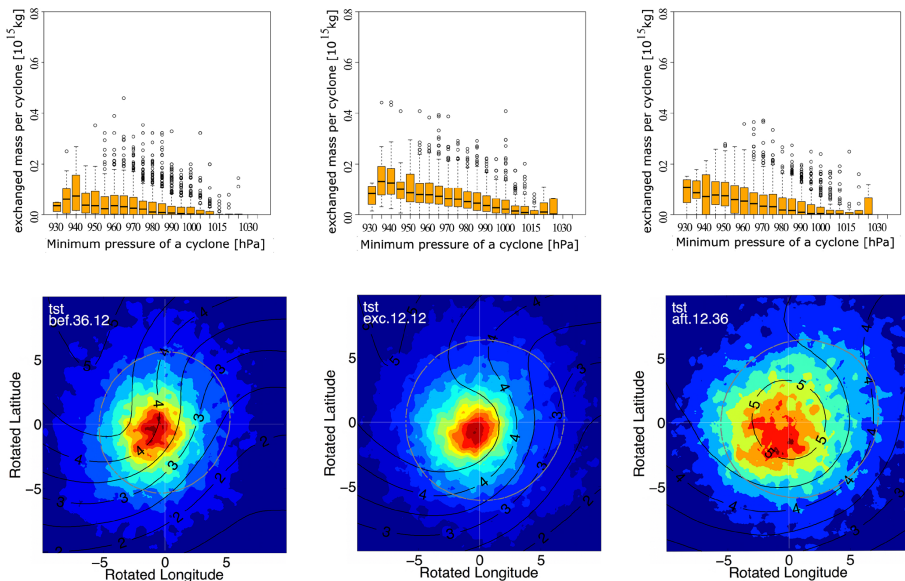


Figure 10. As Fig. 9 but for TST instead of STT.

Title Page

Abstract

Introduction

Conclusions

References

Tables

Figures

